https://doi.org/10.5194/egusphere-2025-5778
Preprint. Discussion started: 11 December 2025

Ecosystem respiration during snowmelt and soil thaw leads to a rare annual CO_2 net loss in a boreal fen

Karoliina Särkelä[1], Timo Vesala[2], Torben R. Christensen[1,3], Juval Cohen[4], Angelika Kübert[2], Xuefei Li[2], Hannu Marttila[1], Jouni Pulliainen[4], Eeva-Stiina Tuittila[5], Efrén López-Blanco[3,6]

[1] Water, Energy and Environmental Engineering Research Unit, University of Oulu, Oulu, Finland
[2] Institute for Atmospheric and Earth System Research, University of Helsinki, Helsinki, Finland
[3] Department of Ecoscience and Arctic Research Centre, Aarhus University, Roskilde, Denmark
[4] Finnish Meteorological Institute, Helsinki, Finland
[5] School of Forest Sciences, University of Eastern Finland, Joensuu, Finland
[6] Department of Environment and Minerals, Greenland Institute of Natural Resources, Nuuk, Greenland

Correspondence to: karoliina.sarkela@oulu.fi

Abstract. Although boreal peatlands play a critical role in the global carbon cycle, their year-round carbon dioxide (CO_2) dynamics — and particularly the contribution of the non-growing season (NGS) — remain poorly constrained in annual balance estimates. Using 17 years (2005–2021) of eddy covariance measurements from a fen in southern Finland, we first quantified the magnitude, timing, and interannual variability of CO_2 fluxes. We then examined in greater detail the NGS, with particular emphasis on soil temperature dynamics and the role of thermal legacy effects. On average, the NGS accounted for 60% of the year (226 ± 27 days), ranging from mid-September to late April, and offset 57% of the subsequent growing season's (GS) CO_2 uptake. NGS emissions declined from autumn to spring, with the highest carbon emissions occurring across September–December and the lowest in January–February. Soil temperature—both concurrent and lagged up to four months—was the main control of CO_2 fluxes during November–December and spring thaw, while photosynthetically active radiation (PAR) dominated during the onset of the NGS. Variability in annual CO_2 balances was large, and in two years (2016 and 2018) the fen switched from a net CO_2 sink to a source. Finally, we focused on 2016 in detail: an exceptional six-week CO_2 release during April–May released 84 g C m^{-2}, offsetting 38% of the following GS CO_2 uptake. This event was linked to unusually warm late-autumn soils, minimal snow insulation, and subsequent rapid surface freezing, which likely enhanced CO_2 accumulation and stimulated CO_2 release during thaw. Our results demonstrate that short-lived but intense NGS events can determine the annual peatland CO_2 balance and therefore significantly affect the annual carbon budget of boreal peatlands.

1 Introduction

Boreal and sub-Arctic peatlands store between 400 Gt (Gorham, 1991; Yu et al., 2011) and 1,000 Gt of carbon (Nichols & Peteet, 2019), contributing up to 30% of the global soil carbon pool (Friedlingstein et al., 2022). These ecosystems have had a

https://doi.org/10.5194/egusphere-2025-5778
Preprint. Discussion started: 11 December 2025

net cooling effect on the atmosphere over the past millennia, as carbon uptake by plants has outweighed losses from heterotrophic respiration (Hugelius et al., 2020). However, global warming — especially at high latitudes, where temperatures are rising three to four times faster than the global average (AMAP, 2021; Rantanen et al., 2022) — may alter the balance between carbon sequestration and loss in boreal and sub-Arctic regions. Elevated temperatures have already intensified carbon cycling by enhancing both productivity and respiration in these ecosystems (See et al., 2024).

Carbon dynamics outside the growing season (GS), i.e., late autumn, winter, and early spring, play a critical yet understudied role in shaping the annual carbon balance of boreal peatlands. These non-growing season periods have become increasingly important as warming trends intensify during the coldest months (Rantanen et al., 2023). While fluxes are typically low in mid-winter, cumulative emissions can offset a significant proportion of growing season uptake, with up to three-quarters of summer sequestration negated in some years based on in situ measurements in the boreal–Arctic zone (Arndt et al., 2023; Virkkala et al., 2022). These emissions are expected to increase even further in the future (Natali et al., 2019), linked with decreasing snow depth and snow cover duration (Pongracz et al., 2024).

Carry-over effects from previous seasons can strongly influence CO_2 fluxes during the non-growing season. For example, high microbial activity during warm summer and autumn can lead to gas build-up in the soil, which is then subsequently released during soil freeze-up or thaw (Raz-Yaseef et al., 2017; Sullivan et al., 2012). Pulses of high carbon release during freezing and thawing have been observed for both methane (Mastepanov et al., 2013) and CO_2 (Raz-Yaseef et al., 2017; Arndt et al., 2020; Wang et al., 2023). These events, though infrequent, have been shown to have the potential to reduce annual carbon uptake by up to 46% (Raz-Yaseef et al., 2017), highlighting the importance of understanding carbon exchange across the full annual cycle.

Despite their non-trivial implications for net carbon sink strength, NGS processes remain underrepresented in carbon flux studies, largely due to logistical and environmental challenges. Data from the ABCFlux database show that the majority of flux measurements still occur during the growing season, with June to August accounting for 32% of observations, compared to just 18% for winter (Virkkala et al., 2022; Virkkala et al., 2025; See et al., 2024). Eddy covariance (EC) sites provide high-temporal-resolution measurements of atmosphere–biosphere exchanges at the ecosystem scale and are the only method capable of directly quantifying net carbon fluxes across these areas. However, relatively few EC sites operate continuously year-round (Pallandt et al., 2022), leaving major gaps in our understanding of winter emissions and seasonal transitions (Hugelius et al., 2024).

This study utilizes a unique 17-year (2005–2021) time series dataset (Alekseychik et al., 2024) of the net ecosystem exchange of CO_2 (NEE) from the Siikaneva fen to understand the overall interannual variability and examine the role of non-growing

https://doi.org/10.5194/egusphere-2025-5778
Preprint. Discussion started: 11 December 2025

season periods in the annual carbon balance of a boreal fen. Given the scarcity of long-term, year-round measurements, this study offers a rare dataset for assessing long-term carbon exchange in these ecosystems.

The aim of this study is to assess the no-growing season (NGS) carbon exchange and identify periods within the NGS that contributed significantly to the annual carbon balance. We specifically ask:

1. How much does the NGS contribute to the annual CO_2 balance in the Siikaneva fen, and what are the seasonal patterns of CO_2 fluxes during the NGS?
2. What are the primary environmental drivers of CO_2 fluxes during the NGS? Specifically, do prior soil thermal conditions predict NGS fluxes, particularly during high-emission periods?

We hypothesize that the NGS contributes substantially to the annual CO_2 balance, with distinct seasonal patterns characterized by higher emissions in autumn and spring thaw periods. We expect soil temperature to be the primary driver of NGS CO_2 fluxes, with soil thermal conditions from prior seasons potentially affecting CO_2 exchange, especially during late autumn and spring soil thaw.

2 Methods

2.1 Site description

Siikaneva wetland (Fig. 1) study site is an oligotrophic fen within a large aapamire complex located in southern Finland (61°50′N, 24°12′E, 162 m above sea level), with ongoing measurements since 2005. The site has been part of the ICOS research infrastructure since 2017 and is classified as a Class 2 ecosystem station. Peat depth at the site ranges from 2 to 6 meters. The terrain is generally flat, with vegetation dominated by peat mosses (*Sphagnum balticum* [Russow] C.E.O. Jensen, *S. majus* [Russow] C.E.O. Jensen, *S. papillosum* Lindb.), sedges (C*arex rostrata* Stokes, *C. limosa* L., *Eriophorum vaginatum* L.), and Rannoch rush (*Scheuchzeria palustris* L.) (Korrensalo et al., 2024). On one site the fen is neighboured by Scots pine forest growth on mineral soil. The mean annual temperature for the period 1971–2000 was 3.3°C, and the total annual precipitation was 713 mm, based on data from the Hyytiälä weather station, located 5 km from Siikaneva (Drebs et al., 2002).

https://doi.org/10.5194/egusphere-2025-5778
Preprint. Discussion started: 11 December 2025

Figure 1. Photo composite featuring Siikaneva in September (left), December (middle) and July (right). Photos by Maximilian King and Karoliina Särkelä.

2.2 Definition of non-growing and growing seasons

Many different definitions exist for the growing season (GS) and non-growing season (NGS), which can be based on environmental variables such as air temperature (referred to as the thermal growing season when persistently above 5 °C (Kollo et al., 2023)), snow cover period (Arndt et al., 2020; Rafat et al., 2022), or thresholds in gross primary production (Böttcher et al., 2014). In this study, we define GS and NGS based on the ecosystem carbon exchange (NEE), following one of the definitions suggested by Körner et al. (2023). The GS corresponds to the period when the ecosystem acts as a net carbon sink (daily NEE < 0), and the NGS when it is a net carbon source (daily NEE > 0). We used a threshold of three days (following the sink period definition by Aurela et al. (2004)): the GS starts on the first of three consecutive days with negative NEE and ends on the first of three consecutive days with positive NEE. mention Thermal growing season (Kollo et al., 2023) when air temperature is persistently above 5 °C.

2.3 Eddy covariance (EC) measurements

The net ecosystem exchange (NEE) of CO_2 at the Siikaneva fen site was measured using the eddy covariance (EC) technique (Baldocchi et al., 2003), providing continuous, high-frequency estimates of ecosystem–atmosphere CO_2 exchange. Measurements have been conducted since 2005, with the flux tower installed at a height of 2.7 m above the peat surface. The

https://doi.org/10.5194/egusphere-2025-5778
Preprint. Discussion started: 11 December 2025

75 % flux footprint corresponds to an area of approximately 200 m radius around the tower (Riutta et al., 2007). Between 2005 and 2015, the EC system consisted of a Metek USA-1 three-dimensional sonic anemometer (Metek GmbH, Elmshorn, Germany) and a LI-COR LI-7000 CO_2/H_2O gas analyzer (LI-COR, Lincoln, NE, USA). In late 2015, the system was upgraded to a Gill HS-50 anemometer (Gill Instruments Ltd., UK) and a LI-COR LI-7200 enclosed-path gas analyzer, resulting in a data gap between September 2015 and February 2016.

Raw 10 Hz data were processed in EddyUH (Mammarella et al., 2016), including despiking, double coordinate rotation, sonic temperature correction, frequency response correction, and the Webb–Pearman–Leuning density correction. Fluxes were filtered for turbulence intermittency and atmospheric stability and corrected for CO_2 storage below the measurement height. Further details on EC data processing can be found in Mammarella et al. (2016). Missing NEE data was gapfilled with the sum of modelled gross primary productivity (GPP) and ecosystem respiration (Reco). GPP was modelled as a function of photosynthetically active radiation (PAR) and air temperature, with parameters optimized for each time period. Photosynthesis was constrained to zero when air temperature dropped below 0 °C. Reco was modelled as a function of air temperature using site- and period-specific coefficients. The equations for the flux partitioning are provided in Kulmala et al. (2019) with site-specific modifications – for the flux timeseries in Siikaneva fen, air temperature was used to model the Reco as soil temperature records were inconsistent across the study period. Processed and gap-filled hourly NEE data were aggregated to daily sums and converted from µmol CO_2 m^{-2} s^{-1} to g C m^{-2} d^{-1}. Negative NEE values indicate net ecosystem carbon uptake.

2.4 Ancillary measurement

We reviewed a range of ancillary environmental variables alongside CO_2 fluxes, including soil temperature, photosynthetically active radiation (PAR), vapor pressure deficit (VPD), precipitation, water table depth, and snow depth.

Soil temperature was measured using Campbell 107 thermistors (Campbell Scientific, Logan, UT, USA) from 2005 to 2016, and UMS TH3-s temperature profile probes (UMS GmbH & Co. KG, Willmars, Germany) from 2017 to 2021. The latter represents the average of five microsites within the EC footprint. Data from 5 and 50 cm depths (2005–2016) and from 5 and 45 cm depths (2017–2021) were used, specifically from a lawn microsite representative of the EC footprint. For consistency, temperatures at 45 cm and 50 cm are both referred to as "soil temperature at 50 cm depth." Photosynthetically active radiation (PAR, µmol/m²) was measured with a Li-Cor Li-190R quantum sensor (LI-COR, Lincoln, NE, USA), but data from 2009–2015 were excluded due to sensor malfunction. Data from the Hyytiälä forestry site (5 km to the northeast of Siikaneva) were used for this period, measured with a Li-Cor Li-190SZ quantum sensor (LI-COR, Lincoln, NE, USA). Vapor pressure deficit (VPD, kPa) was calculated using the fCalcVPDfromRHandTair function in the R package ReddyProc (Wutzler et al., 2022), based on air temperature and relative humidity from a Rotronic HC2 sensor (Rotronic AG, Bassersdorf, Switzerland). Water table depth (WTD) was measured with Druck PDCR1830 and Campbell CS451 pressure transducers (Campbell Scientific). WTD is expressed in centimeters (cm) relative to the surface, with negative values indicating depths below ground. Precipitation (mm) was recorded using an ARG-100 tipping bucket rain gauge (2005–2016), which underreports sleet and

https://doi.org/10.5194/egusphere-2025-5778
Preprint. Discussion started: 11 December 2025

snow. In 2017, it was replaced by an OTT Pluvio2S weighing rain gauge (OTT HydroMet, Kempten, Germany). Instrument upgrades in late 2015 caused data gaps across several variables (dates vary by parameter). To assess autumn and winter 2015 conditions, air temperature and snow depth data were retrieved from the Hyytiälä Forestry Station, 5 km from Siikaneva. Air temperature there was measured with a Pt100 sensor inside a custom shield. A linear regression comparing air temperatures at the two sites yielded a slope of 0.98 and R^2 of 0.98, validating the use of Hyytiälä's temperature data.

2.5 Freeze–thaw status classification

The freeze–thaw state of the study area was classified using the Sentinel-1 IW GRD SAR (Synthetic Aperture Radar) data available from autumn 2014 onwards. These data have been processed by Google Earth Engine into calibrated and ortho-rectified grids of Sigma Nought backscatter values with 10 m pixel size. Median backscatter time series (VV, VH, and VH/VV ratio) were extracted for a 200 m zone around the Eddy Covariance mast and the broader Siikaneva Fen. Data from both ascending and descending orbits were used. Freeze–thaw periods were identified through visual inspection of backscatter trends, supported by in situ measurements (air and soil temperature, soil water content, and snow depth). Due to changes in liquid water content, soil freezing typically reduces the measured backscatter intensity by a few decibels, and the presence of wet snow further reduces the backscatter by an additional few decibels. Freezing onset was marked by a ≥2 dB drop in backscatter in VV polarization; the frozen period ended when all orbits consistently showed low values. Thaw onset was defined either by a sharp drop indicating wet snow or by a rise in backscatter consistent with thawed soil; thaw ended when all orbits showed higher backscatter values typical of thawed conditions.

2.6 Data analysis

We quantified the relative importance of environmental drivers controlling the carbon sink or source strength, expressed as daily net ecosystem exchange (NEE), using a machine-learning random forest regression algorithm. Random forest is a machine-learning technique widely used for complex multi-regression analyses (e.g., López-Blanco et al., 2017 and 2020; Wei et al., 2021) that builds an ensemble of decision trees by repeatedly sampling random subsets of the training data (Breiman, 2001; Pedregosa et al., 2011). Each decision tree partitions the explanatory variables (covariates) to create clusters of data, within which regression models predict the response variable (NEE). Variable importance is then quantified as the percentage of times a variable is used in the decision splits across all trees, reflecting its contribution to explaining variability in NEE.

Our set of explanatory variables included photosynthetically active radiation (PAR), vapor pressure deficit (VPD), water table depth (WTD), and soil temperature. All variables and NEE were aggregated to daily means. Daily data were then binned into two-month periods: January–February, March–April, May–June, July–August, September–October, and November–December. These periods loosely follow the approximate periods when the system turns into a net source, i.e., the onset of the NGS (September–October); when the surface freezes (November–December); when the surface is typically frozen (January–February); when the surface thaws (March–April); when the system turns into a net sink of CO_2, i.e., the onset of the GS (May–

https://doi.org/10.5194/egusphere-2025-5778
Preprint. Discussion started: 11 December 2025

June); and when it is consistently a net sink of CO_2 (July–August). Variable importance was then assessed for each model, with standard deviations calculated to evaluate uncertainty.

Days with fewer than 12 hourly NEE observations were excluded from the analysis to ensure data quality. Due to incomplete PAR records at the Siikaneva site for 2009–2015, PAR data from the nearby Hyytiälä Forest Station (5 km to the northeast of the Siikaneva fen) were used as a proxy. Due to strong collinearity between air temperature and soil temperature, we did not include air temperature in the analysis. Precipitation was excluded as an explanatory variable, since the instrument measuring precipitation could not reliably detect snow and sleet. Therefore, such precipitation data could introduce biases in the analysis by underestimating the amount of precipitation during winter compared to summer.

To investigate the potential influence of soil thermal conditions over different temporal scales and legacy effects, three separate model frameworks were constructed, each differing in how soil temperature was aggregated:
(A) Daily mean soil temperature at 5 cm depth, representing contemporaneous conditions.
(B) Daily running mean of 60 days of soil temperature at 5 cm, representing the conditions in the last two months.
(C) Daily running mean of 60 days of soil temperature at 5 cm, lagged by 60 days, representing the conditions 2–4 months prior. For example, the soil temperature data point used as a driver for the daily NEE on 1 April is the mean soil temperature between 2 December and 30 January.

3 Results

3.1 Duration of NGS

On average, the non-growing season (NGS) accounted for 60% (226 ± 27 days) of the year, beginning on September 17th (±19 days) and ending on April 30th (±15 days). The NGS started latest in 2011 on October 26th and earliest in 2018 on July 30th (Fig. 2a). The NGS ended the earliest in 2006 on March 18th and latest in 2016 on June 2nd (Fig. 2a). The NGS that started in 2018 and ended in 2019 was the longest NGS (278 days) in the whole study period, due to an exceptionally early start of the season.

https://doi.org/10.5194/egusphere-2025-5778
Preprint. Discussion started: 11 December 2025

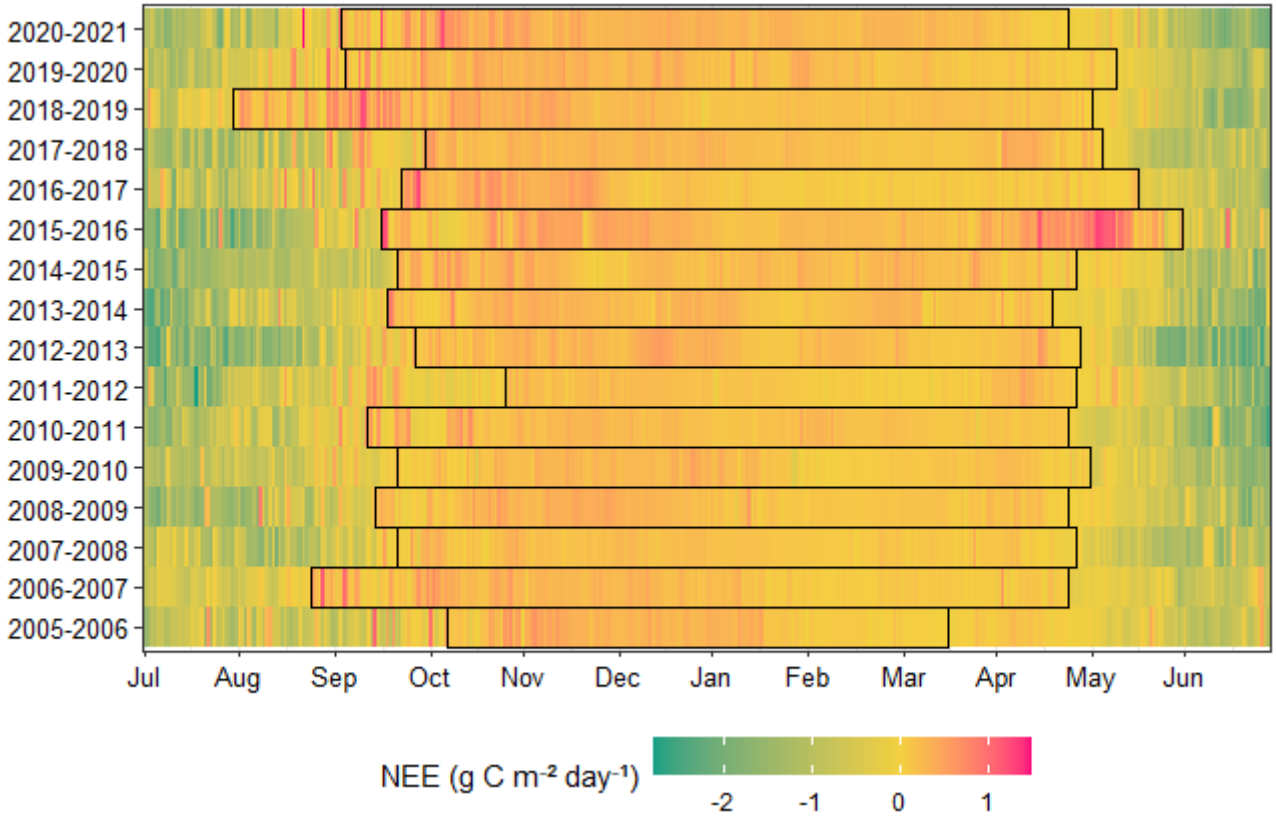

Figure 2. (A) Daily net ecosystem exchange of CO_2 (NEE; g C m^{-2} day^{-1}) in 2005–2021 and the non-growing season (NGS, black rectangular outline) periods centered in the winter. Each row represents one year, beginning in July and ending in June of the following year. Colors indicate daily mean NEE values, where the yellow–green gradient reflects negative values (net carbon sink) and the yellow–pink gradient reflects positive values (net carbon release). Black rectangular outlines mark the NGS periods, defined as the period beginning after the first three consecutive days of positive NEE and ending after the first three consecutive days of negative NEE. On average, the NGS started on September 17th and ended on April 30th.

3.2 Interannual and interseasonal CO_2 fluxes

The fen acted as a net CO_2 sink during the study period, with an average annual uptake of –51 ± 39 g C m^{-2}. In two years, 2016 and 2018, the fen was a net source of CO_2, releasing 28 g C m^{-2} and 21 g C m^{-2}, respectively (Fig. A1a). However, when looking at the pairs of full NGS and GS (Fig. 3a), only GS 2016 and the preceding NGS from 2015–2016 were a net source of CO_2. The mean cumulative carbon release during the NGSs was 49 ± 15 g C m^{-2} (Fig. 3a), offsetting on average 57% of the following GS's carbon uptake (–100 ± 31 g C m^{-2}) (Fig. 3a). Interannual variability was high (±33%). The lowest cumulative carbon emissions over the NGS were observed in 2012 (26 g C m^{-2}), while the highest were recorded in 2016 (84 g C m^{-2}) (Fig. 3a). The mean daily CO_2 flux during NGS ranged from 0.14 g C m^{-2} in 2012 to 0.33 g C m^{-2} in 2016. Mean during the whole study period was 0.21 ± 0.048 g C m^{-2}.

https://doi.org/10.5194/egusphere-2025-5778
Preprint. Discussion started: 11 December 2025

During the NGS, CO_2 emissions generally declined from autumn to spring (Fig. 3a and 3b). The transitional months of October and April, marking the shift into and out of the growing season, showed the highest interannual variability (Fig. 3a and 3b). Emissions peaked in November (9.03 ± 2.07 g C m^{-2}), followed by October (8.09 ± 3.60 g C m^{-2}) and December (7.9 ± 2 g C m^{-2}; Fig. 3b). Mean CO_2 emissions during October–December were significantly higher than those in January–March (8.4 vs. 4.8 g C m^{-2}; Fig. 3b). April and May of 2016, both part of the NGS that year, exhibited the highest monthly net CO_2 losses and the largest deviations from the long-term mean, followed by August and September in 2018 (Fig. 3a and 2b). Fluxes during that 2016 period exceeded the 95th percentile for 32 nearly consecutive days (see Fig. S5 in the Supplement). All other periods with three or more consecutive days above the 95th percentile occurred between September and December, with event durations of up to five days (see Fig. S5 in the Supplement).

The strongest CO_2 sinks occurred in June and July (-33 ± 9.6 g C m^{-2} and -33 ± 11 g C m^{-2}, respectively; Fig. 3B). Monthly variability was higher during periods of net CO_2 sink (May–September; Fig. 3b) than during the NGS.

There was a significant data gap in the EC measurements from September 22, 2015, to February 25, 2016. Notably, 2016 had the highest annual carbon emissions (January 1–December 31, Fig. A1a). To ensure that this finding was not an artifact of the extended gap-filled period, annual balances were recalculated for all years, excluding data from January 1 to February 25 (Fig. A1b). Since 2016 still showed the highest annual balance (meaning a net source of CO_2), we conclude that the gap-filling procedure did not significantly bias the results.

https://doi.org/10.5194/egusphere-2025-5778
Preprint. Discussion started: 11 December 2025

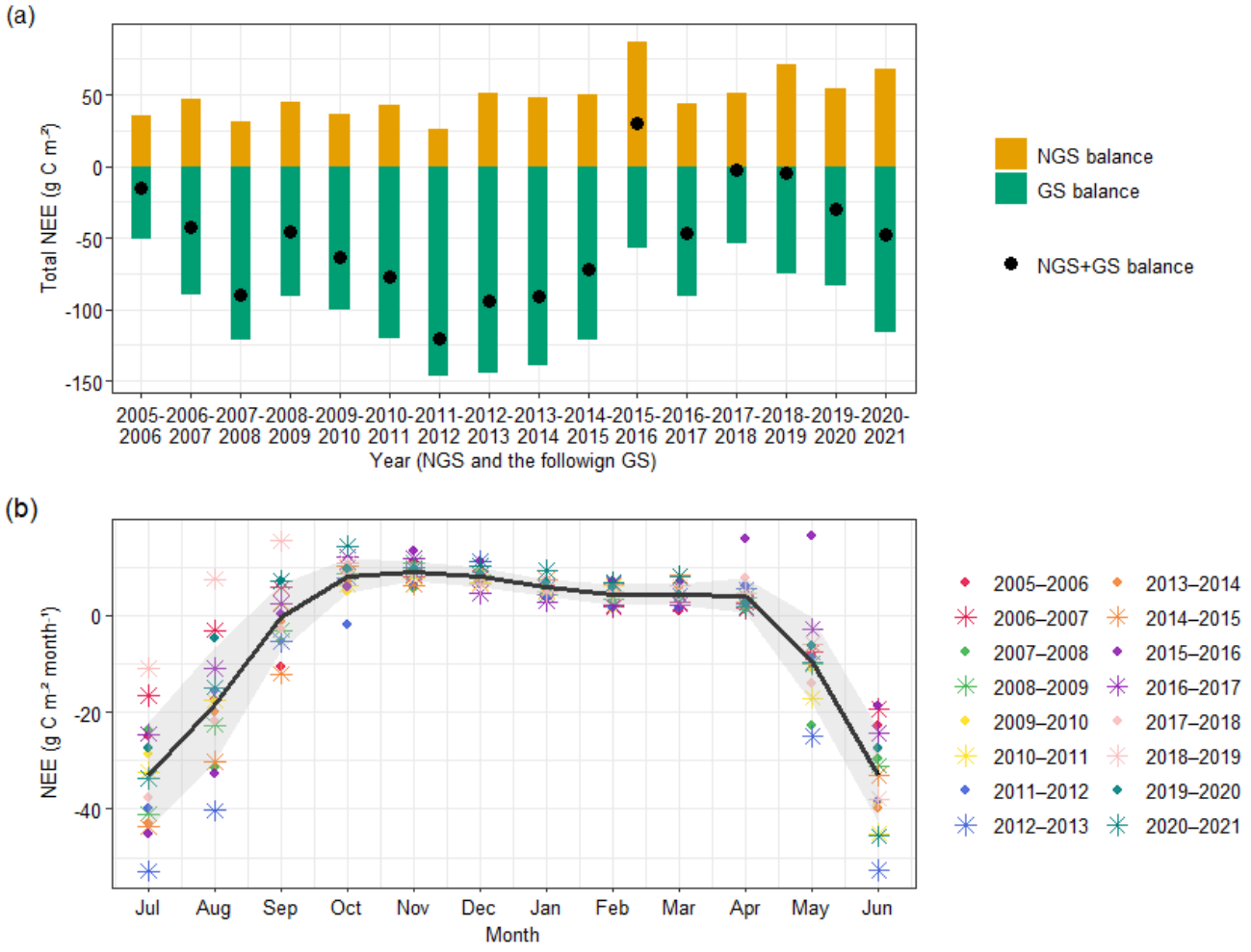

Figure 3. (a) Non-growing season (NGS) and growing season (GS) net ecosystem exchange (NEE) sums of CO_2 for each full NGS and the following GS, with the net balance of the combined period indicated by black points. Negative values indicate a carbon uptake and positive values indicate carbon loss to the atmosphere. We use the terms growing season (GS) and non-growing season (NGS) to refer to periods when the ecosystem acts as a net carbon sink (GS) or a net carbon source (NGS), based on daily NEE values, following the definition for a sink period by Aurela et al. (2004). The start of the NGS is defined as the first of three consecutive days with positive NEE, and the GS begins on the first of three consecutive days with negative NEE. The NGS sum of CO_2 is calculated for the full season, starting in autumn and ending in spring. (b) Monthly NEE sums across the study years, with the mean monthly sums (black line) and standard deviation (shaded area) shown for the period 2005–2021.

3.3 Respiration release in spring 2016

Since 2016 exhibited the highest cumulative CO_2 emissions during the non-growing season (84 g C m^{-2}) and was one of the few years with an annual net carbon loss (28 g C m^{-2}), coupled with unusually high net emissions of CO_2 in April and May

https://doi.org/10.5194/egusphere-2025-5778
Preprint. Discussion started: 11 December 2025

(Fig. 3b), we examined this year in greater detail to better understand the underlying drivers and the conditions leading up to and during the peak emission period (Fig. 4).

The late autumn of 2015 was notably warm, with November-October reaching the highest mean temperature in the 2005–2021 record at 1.69 °C, 3.22 °C above the long-term average (Fig. 4c). A sharp temperature drop in January 2016 drove surface soil temperatures to their lowest levels recorded from 2005 to 2021, with air temperatures plunging from above zero to –25 °C over a two-week period (Fig. 4c). The cold spell lasted nearly three weeks, and the second-lowest air temperature in the study period (–25.2 °C) was recorded. Snow depth was not measured for most of the winter in early 2016 at Siikaneva. Measurements at Hyytiälä (5 km to the northeast of Siikaneva) recorded no snowpack at the beginning of the cold spell. During the cold spell, snow depth only increased from 0 to 4 cm—well below the 2016–2021 average of 16 cm. Surface soils froze, but the deeper soil layers remained warmer throughout the winter (Fig. 4b) due to the warm late autumn. From January to March 2016, the mean soil temperature at 50 cm depth was about 0.85 °C higher than the long-term at 2.95 °C. The soil temperature showed unique fluctuations at 50 cm depth but not in shallower layers (Sup. Fig. 2).

Complementary satellite-derived freeze–thaw status classification indicated the beginning of thawing for the 200 m radius from the EC mast on March 27th, marking the start of snowmelt (see Table S2 in the Supplement). At this point, CO_2 flux increased sharply while soil temperatures at 5 cm remained at 0 °C (Fig. 4a–b). These elevated emissions persisted throughout the entire thawing period. Once the soil temperature at 5 cm began to rise more rapidly, a second, more pronounced peak in NEE emissions followed, fluctuating in response to the warming topsoil (Fig. 4a–b). In April 2016, daily emissions (positive NEE) were nearly four times higher than the monthly average—0.53 g C m^{-2} d^{-1} compared to the typical 0.13 g C m^{-2} d^{-1}. Cumulative emissions in April and May were substantial, offsetting 38% of the total carbon uptake observed during the subsequent growing season.

https://doi.org/10.5194/egusphere-2025-5778
Preprint. Discussion started: 11 December 2025

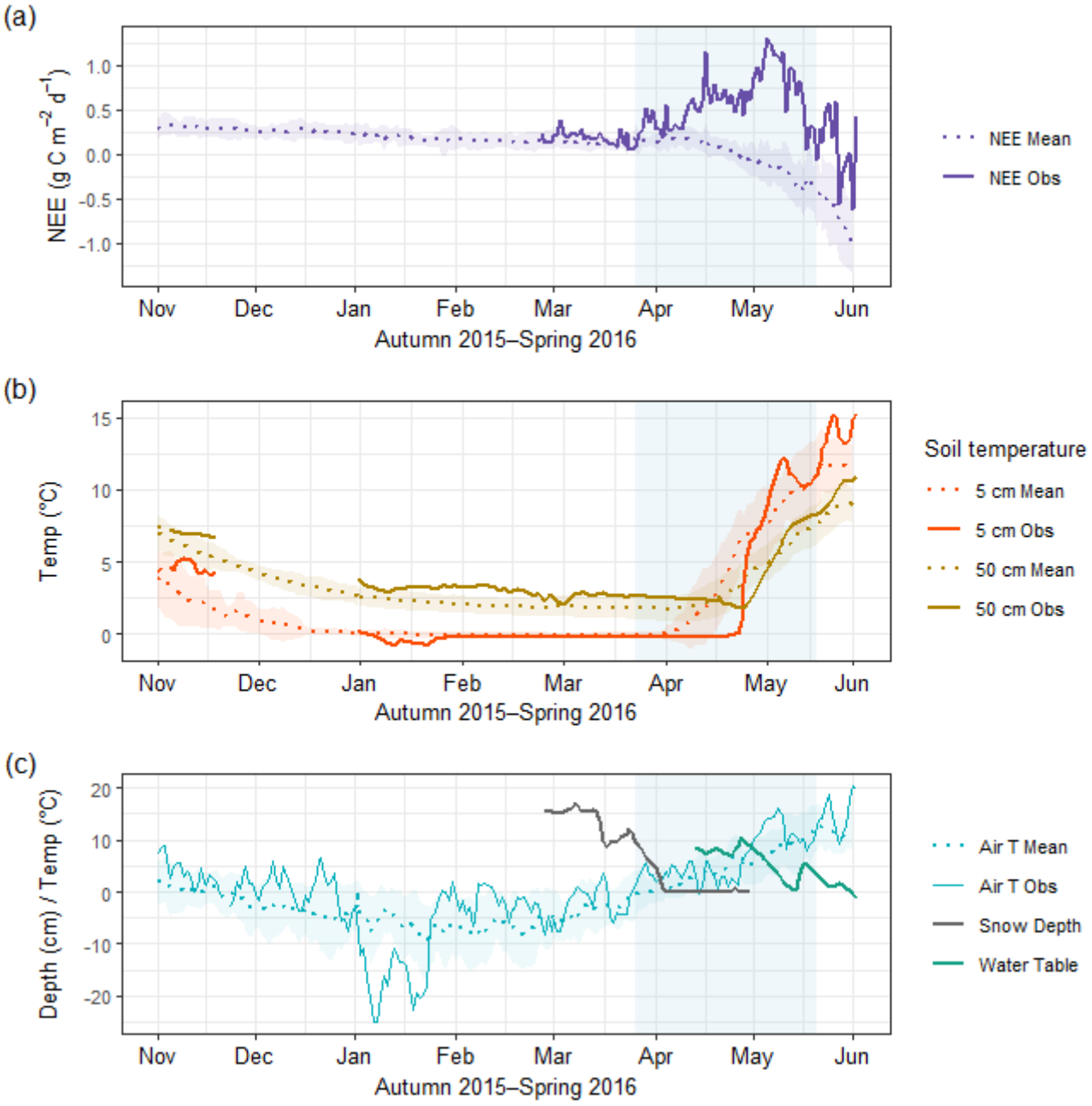

270 **Figure 4.** (a) Daily means of Net Ecosystem Exchange of CO_2, (b) soil temperature at 5 cm and 50 cm depth, and (c) air temperature, snow depth, and water table depth (expressed as centimeters from the surface, where positive values indicate water level above the surface) from November 1st, 2015, to June 1st, 2016. In each panel, the solid line shows observed values, the dotted line represents the mean for each day of the year (2005–2021, excluding 2015–2016), and shading indicates the standard deviation. Air temperature was measured 9 km

https://doi.org/10.5194/egusphere-2025-5778
Preprint. Discussion started: 11 December 2025

away at the Hyytiälä Forest Station due to a data gap at the Siikaneva site in autumn 2015. The blue shading highlights the period of high flux values observed in spring 2016.

3.4 Variable importance controlling NEE

We used machine learning random forest models to evaluate the relative importance of environmental drivers controlling CO_2 exchange, with a particular focus on the role of soil temperature over different time scales. The pronounced respiration pulse observed in spring 2016 (Fig. 4a) suggested that soil thermal conditions from the preceding autumn and winter (Fig. 4b) might influence carbon emissions during soil thaw. To investigate this, we compared three temporal representations of soil temperature as predictors: concurrent daily soil temperature (Fig. 5a), a 60-day running mean (Fig. 5b), and a 60-day running mean lagged by two months (Fig. 5c). The 60-day window was chosen to capture potential cross-seasonal effects of soil temperature, such as the influence of summer conditions on autumn respiration and late-autumn temperatures on winter CO_2 efflux.

Random forest models that were used to evaluate the relative importance of environmental drivers controlling CO_2 exchange revealed that during soil thawing and snowmelt in March–April (see Fig. S4 in the Supplement), fluxes were influenced by both concurrent soil temperature (Fig. 5a) and the thermal history (Fig. 5b and 4c) of the preceding four months. Concurrent soil temperature dominated fluxes during the highest non-growing season emissions in November–December (38 % ± 5.2; Fig. 5a). At the onset of the non-growing season (September–October), CO_2 exchange was primarily driven by PAR (58 % ± 3.1 %; Fig. 5a). During January–February, when soils were typically frozen or snow-covered (see Fig. S4 in the Supplement), no single driver clearly dominated (Fig. 5a). During the GS, fluxes were mainly driven by PAR (43 % ± 3.4 %; Fig. 5a) and WTD (36 % ± 3.2 %; Fig. 5a). The soil thermal conditions in the last 60 days were also an important driver during the onset of the GS (Fig. 5b).

https://doi.org/10.5194/egusphere-2025-5778
Preprint. Discussion started: 11 December 2025

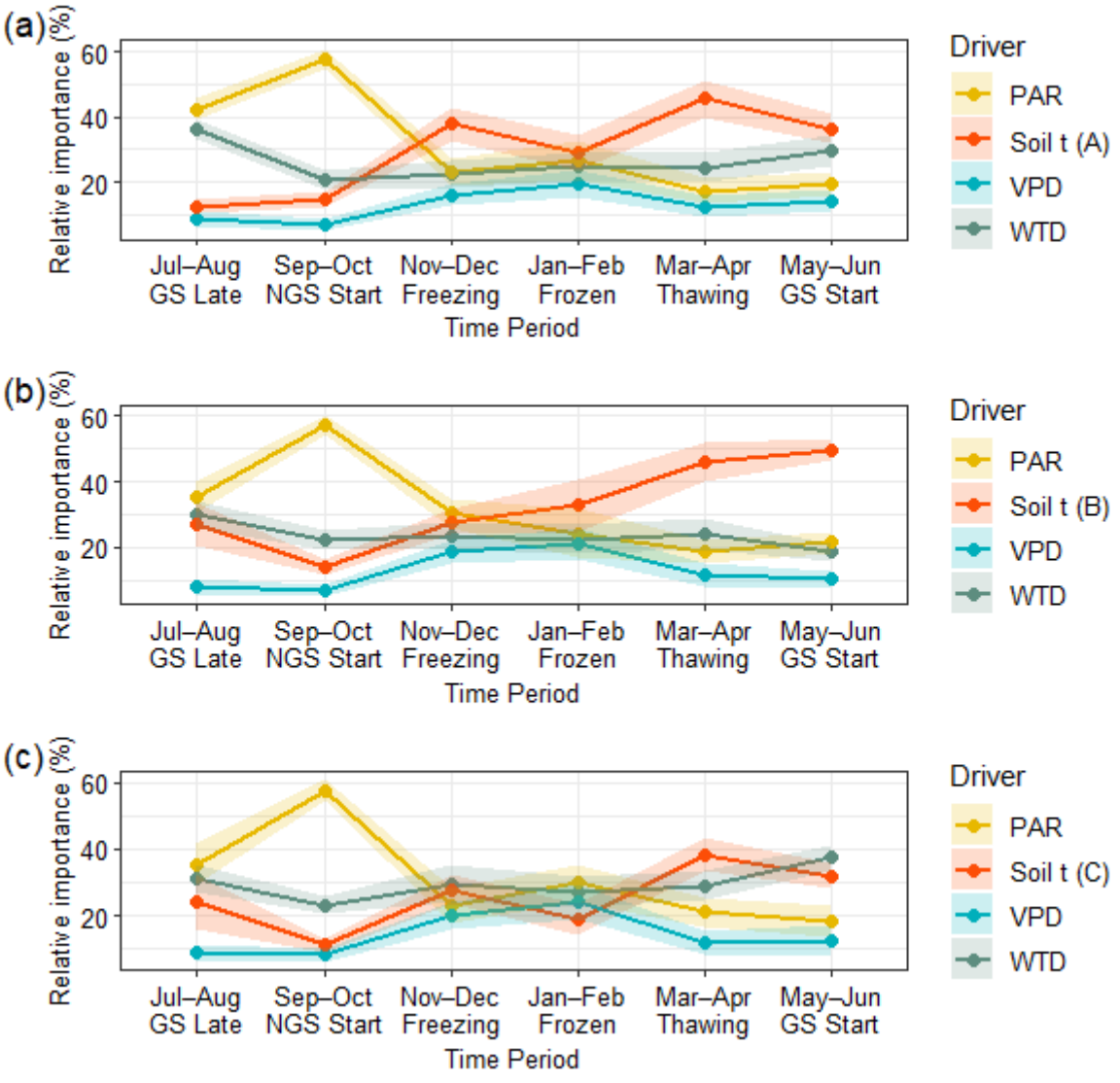

Figure 5. Relative importance of photosynthetically active radiation (PAR), vapor pressure deficit (VPD), water table depth (WTD), and soil temperature at 5 cm in predicting daily net ecosystem exchange (NEE), based on random forest models. All variables and NEE were aggregated to daily means. Shading represents standard deviation. Due to incomplete PAR records at the Siikaneva site, data from the Hyytiälä Forest Station were used for 2009–2015. Subplots differ in the soil temperature aggregation used: a) Daily mean soil temperature at 5 cm; b) Mean soil temperature at 5 cm, averaged over the two months preceding each flux measurement; c) Mean soil temperature at 5 cm, averaged over a two-month window and lagged by 60 days (i.e., a lagged two-month mean).

https://doi.org/10.5194/egusphere-2025-5778
Preprint. Discussion started: 11 December 2025

4 Discussion

Our aim is to examine how much the NGS contributed to annual CO_2 exchange at the Siikaneva fen and to describe the seasonal patterns of CO_2 fluxes during this period. Additionally, we investigated the main environmental factors driving CO_2 emissions in the NGS, specifically focusing on concurrent and lagged soil temperature as a driver during the NGS. The year 2016 emerged as a key focus because it featured an unusually large CO_2 release during the spring thaw.

4.1 Annual, NGS, and GS carbon exchange

On average, the studied fen ecosystem functioned as a CO_2 sink, with an annual net carbon uptake of -51 ± 39 g C m^{-2}. This is more than twice the mean of boreal wetlands based on a recent synthesis (-17 g C m^{-2} yr^{-1}; Virkkala et al., 2021), indicating it is a highly productive wetland site. Emissions during the NGS offset approximately 60% of the carbon sequestered during the following GS (Fig. 3A), a proportion comparable to that observed in other wetland sites (Virkkala et al., 2021; Aurela et al., 2002; Wang et al., 2023; López-Blanco et al., 2018; Yao et al., 2022), although based on different NGS definitions.

The NGS lasted on average from mid-September through the end of April (Fig. 2). Emissions during the NGS generally declined from autumn to spring (Fig. 3b): mean fluxes from October to December (8.4 g C m^{-2} mo^{-1}) were nearly twice those observed from January to March. Autumn is typically the period with the highest emissions (Byrne et al., 2022; Commane et al., 2017), which can potentially shift the system to a net carbon source. However, at boreal sites, GS uptake generally offsets autumn emissions, even under current warming trends (See et al., 2024). PAR emerged as a strong driver during September–October, a period when the system typically shifted from GS to NGS. This transition is highly sensitive to declining light availability, which influences the onset and progression of senescence. As a result, day-to-day variability in carbon uptake is largely determined by PAR. During the peak emission period from November to December (Fig. 3b), carbon exchange was mainly controlled by soil temperature (Fig. 5a), which is typically the dominant driver of NGS emissions (Natali et al., 2019).

Emissions were lowest in January and February (Fig. 3b), with low interannual variability and high uncertainty in concurrent environmental drivers (Fig. 5a). This uncertainty may partly arise from a temporal lag between environmental conditions, such as soil temperature, and the observed fluxes, as snow and ice can restrict gas diffusion, allowing CO_2 to build up in the soil and snowpack before being released later (Martz et al., 2016; Morgner et al., 2010). The 60-day averaged soil temperature was also not identified as an important driver (Fig. 5b), indicating that midwinter fluxes are not consistently higher or lower following warmer or colder prior soil conditions.

From March to April, random forest analysis highlighted both concurrent soil temperature and the preceding months' conditions (e.g., the 60-day running mean and December–January soil temperatures) as important predictors of fluxes (Fig. 5). This indicates a legacy effect of late-autumn and early-winter temperatures on spring emissions, consistent with the hypothesis

https://doi.org/10.5194/egusphere-2025-5778
Preprint. Discussion started: 11 December 2025

that CO_2 accumulates during frozen conditions and is released upon thaw (Raz-Yaseef et al., 2017; Sullivan et al., 2012). In addition, thermal conditions in autumn and winter may influence microbial activity and substrate availability during thaw.

4.2 Spring 2016 respiration enhanced by winter conditions and snowmelt

In 2016, an exceptional respiration pulse during April–May dominated the annual CO_2 budget (Fig. 4a). Lasting about six weeks, this event offset 37% of the subsequent GS uptake and produced the highest annual CO_2 loss of the record. Comparable pulses have been reported from other cold-climate wetlands (Wang et al., 2023) and permafrost-affected tundra sites (Raz-Yaseef et al., 2017; Arndt et al., 2020). Raz-Yaseef et al. (2017) and Wang et al. (2023) associated the pulse with the rapid release of gases that accumulated beneath snow and ice during winter. A similar event was reported by Arndt et al. (2020), who further suggested that snowmelt infiltration and oxygen supply can stimulate microbial activity, enhancing respiration during thaw. Our results add to this evidence but are, to our knowledge, the first to document such an event in a non-permafrost site.

During snowmelt, CO_2 emissions rose sharply while surface soil temperatures remained near 0 °C, suggesting release of stored gases from the snowpack and soil, possibly aided by ice cracking (Raz-Yaseef et al., 2017). The random forest analysis confirmed a soil temperature legacy effect, with late-autumn and early-winter conditions influencing fluxes during spring thaw (Fig. 5c). The conditions were favourable for gas buildup in soil during late autumn and winter. Warm conditions in late autumn 2015 and early winter kept deep soil layers relatively warm, promoting CO_2 accumulation. A sharp cold spell in January 2016 then caused rapid surface freezing, likely leading to ice-layer formation that trapped gases. Freezing events can disrupt soil aggregates and microbial communities, exposing labile organic matter that enhances respiration when soils warm in spring (Brooks et al., 2005; Byun et al., 2021; Martz et al., 2016; Morgner et al., 2010), while infiltration of oxygen-rich meltwater may stimulate microbial activity at depth (Arndt et al., 2020), further amplifying respiration during thaw.

Beyond the biological explanations for the 2016 event, a physical process may also be relevant. Campeau et al. (2021) found that weakened thermal stratification in autumn promotes turbulent diffusion that has the potential to release large amount of CO_2 stored in deep porewater to the surface. In our data, temperature fluctuations at 50 cm depth (see Fig. S2 in the Supplement) during winter while the upper layers remained frozen and stable suggest hydrological mixing within saturated peat. The subsequent CO_2 pulse coincided with a period of weak thermal stratification, when the surface and deeper soil layers reached similar temperatures, conditions that could have supported the rapid release of stored CO_2. The pulse may therefore have been supported not only by microbial processes but also by transient physical mixing and mobilization of deeper CO_2. Although direct evidence of porewater CO_2 dynamics is lacking, this temporal correspondence suggests that biological and physical pathways may have interacted to produce the unusually high CO_2 efflux in 2016. More broadly, these findings highlight the need to consider CO_2 accumulation in the peat profile and both vertical and lateral transport as a fully integrated net ecosystem carbon balance (López-Blanco et al., 2025).

https://doi.org/10.5194/egusphere-2025-5778
Preprint. Discussion started: 11 December 2025

Such events appear to be infrequent but can have outsized impacts on the annual carbon balance. In 17 years of monitoring, 2016 was the only year when such a pronounced spring pulse was observed. The event suggests that no single environmental driver can account for its magnitude; rather, several conditions (e.g., warm soils at depth, surface freeze-up) likely needed to coincide for it to occur. To better understand these dynamics, direct monitoring of peat gas buildup during the NGS would be valuable for determining whether spring pulses primarily reflect the release of gases accumulated under frozen conditions or enhanced microbial respiration initiated during thaw.

4.5 Vulnerability of northern wetlands CO_2 balance to NGS changes

The dominance of NGS processes in affecting the annual CO_2 balance means that warming late autumns, earlier spring thaws, or increased frequency of freeze–thaw events could substantially alter the net sink strength of boreal fens. Projected late-season warming may prolong microbial activity and amplify NGS losses (Natali et al., 2019) unless offset by concurrent GS gains (See et al., 2024).

In this time series, two years (2016 and 2018) shifted the fen from a net CO_2 sink to a source (Fig. 3 and Fig. A1). In 2018, a summer drought reduced GS uptake and caused an early NGS onset (Rinne et al., 2020). While this extended the NGS to its longest duration in the record, total NGS emissions remained smaller than in 2016, demonstrating that short-lived but intense NGS events can outweigh more gradual seasonal anomalies in determining the annual carbon balance.

Representation of episodic emissions during spring thaw and autumn freeze is currently lacking in process-based models and future projections (e.g., Watts et al., 2021). Given that high, episodic carbon release during the NGS resulted in the highest annual net loss of CO_2 in this study, models aiming to predict peatland carbon–climate feedbacks must explicitly represent the thermal legacy effects from autumn to spring and soil gas accumulation and release mechanisms during freezing and thawing. Without such process-level representation, predictions may underestimate the potential for short-term NGS events to transform high-productivity peatlands from strong sinks into net sources of CO_2.

5 Conclusions

Our study highlights the importance of NGS carbon exchange in shaping the annual carbon balance of boreal peatlands. While the fen generally acted as a CO_2 sink, episodic events—such as the exceptional spring pulse in 2016—demonstrated that infrequent disturbances can strongly influence the annual carbon balance.

https://doi.org/10.5194/egusphere-2025-5778
Preprint. Discussion started: 11 December 2025

Our results point to the significance of soil thermal history and potential peat gas accumulation as key mechanisms driving these pulses. These processes remain poorly constrained and are not yet well represented in ecosystem models, but they are critical for predicting peatland carbon exchange. Long-term, continuous measurements proved particularly valuable: our 17-year record not only captured infrequent but influential events such as the respiration pulse in 2016 but also provided the broader context to recognize their rarity and evaluate their contribution to interannual variability.

Autumn accounted for the largest share of NGS emissions, emphasizing the role of shoulder seasons in offsetting growing-season uptake. Consequently, warmer autumns and predicted reduced snow cover are likely to enhance CO_2 efflux by prolonging the period of unfrozen soils and stimulating late-season microbial activity.

Looking forward, warming autumns and changes in snow cover will alter soil thermal conditions, which can affect both concurrent CO_2 fluxes during the NGS and fluxes later in the season. Understanding these processes—including soil thermal legacies and potential subsurface gas buildup—is therefore essential for assessing the vulnerability of peatland carbon storage under future climate change.

Data Availability:

The meteorological and soil data (https://doi.org/10.23729/0766621e-99bf-42f2-ad55-889cdb08b66a) and CO_2 flux data (https://doi.org/10.23729/a3c8d0fe-2a69-4aa9-acbd-5da569fd264e) from the SMEAR II Siikaneva fen site during the study period are accessible via the Finnish metadata catalog Etsin.

Appendix A

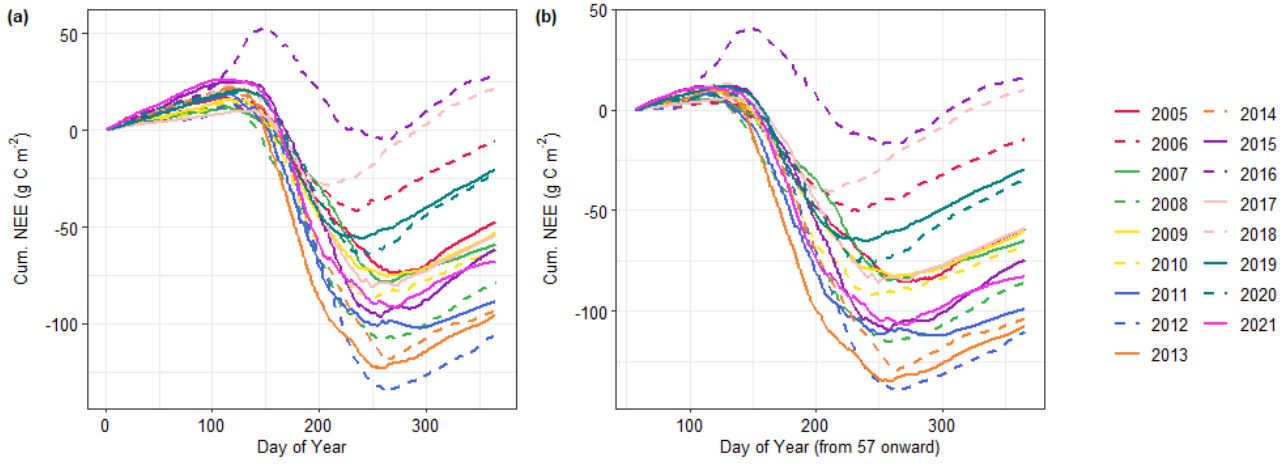

https://doi.org/10.5194/egusphere-2025-5778
Preprint. Discussion started: 11 December 2025

Fig A1. a) Cumulative sums of gap-filled daily sums of net ecosystem exchange of CO2 (NEE), starting from the day of year(DoY) 1 and b) starting from DoY 57 (B). As 2016 had the highest annual balance, but there was a significant measurement gap in DoY 1-57 in 2016, we calculated the annual sums for all years excluding this period. 2016 remained to have the highest balance, and the relative ranking in the annual balances remained similar. We therefore concluded that the positive balance of 2016 was not a result of the gapfilling period.

Author contribution:

KS: Conceptualization, Formal analysis, Investigation, Software, Visualization, Writing (original draft preparation)

TV: Conceptualization, Writing (review and editing)

JC: Methodology and Investigation (section 2.5), Writing (review and editing)

AK: Conceptualization, Writing (review and editing)

XL: Conceptualization, Writing (review and editing)

TRC: Conceptualization, Funding acquisition, Writing (review and editing)

HM: Conceptualization, Writing (review and editing)

EST: Writing (review and editing)

JP: Methodology (Section 2.5)

ELB: Conceptualization, Writing (review and editing)

Competing interests: The authors declare that they have no conflict of interest.

Acknowledgments: We thank the staff and technicians at Hyytiälä Forestry Station for their efforts in maintaining the research infrastructure at the Siikaneva fen. The site is part of the ICOS Finland infrastructure. We acknowledge the use of AI in assisting with code development and text editing. Karoliina Särkelä was supported by the *High-latitude Greenhouse Gases – a Balancing Act (HILAC)* project, funded by the Kvantum Institute, and by the Digital Waters (DIWA) Flagship funded by the Research Council of Finland. Xuefei Li was supported by the Research Council of Finland (Project 371040). ELB and TRC consider this study a contribution to the *GreenFeedBack* project (Greenhouse Gas Fluxes and Earth System Feedbacks), funded by the European Union's Horizon Research and Innovation Programme (Grant Agreement No. 101056921).

References

AMAP. (2021). *AMAP Arctic Climate Change Update 2021: Key Trends and Impacts*. Arctic Monitoring and Assessment Programme (AMAP), Tromsø, Norway.

Arndt, K. A., Hashemi, J., Natali, S. M., Schiferl, L. D., & Virkkala, A.-M. (2023). Recent Advances and Challenges in Monitoring and Modeling Non-Growing Season Carbon Dioxide Fluxes from the Arctic Boreal Zone. *Current Climate Change Reports*, *9*(2), 27–40. https://doi.org/10.1007/s40641-023-00190-4

Arndt, K. A., Lipson, D. A., Hashemi, J., Oechel, W. C., & Zona, D. (2020). Snow melt stimulates ecosystem respiration in Arctic ecosystems. *Global Change Biology*, *26*(9), 5042–5051. https://doi.org/10.1111/gcb.15193

https://doi.org/10.5194/egusphere-2025-5778
Preprint. Discussion started: 11 December 2025

Aurela, M., Laurila, T., & Tuovinen, J.-P. (2002). Annual CO2 balance of a subarctic fen in northern Europe: Importance of the wintertime efflux. *Journal of Geophysical Research: Atmospheres*, *107*(D21), ACH 17-1-ACH 17-12. https://doi.org/10.1029/2002JD002055

Aurela, M., Laurila, T., & Tuovinen, J.-P. (2004). The timing of snow melt controls the annual CO2 balance in a subarctic fen. *Geophysical Research Letters*, *31*(16). https://doi.org/10.1029/2004GL020315

Baldocchi, D. D. (2003). Assessing the eddy covariance technique for evaluating carbon dioxide exchange rates of ecosystems: Past, present and future. *Global Change Biology*, *9*(4), 479–492. https://doi.org/10.1046/j.1365-2486.2003.00629.x

Böttcher, K., Aurela, M., Kervinen, M., Markkanen, T., Mattila, O.-P., Kolari, P., Metsämäki, S., Aalto, T., Arslan, A. N., & Pulliainen, J. (2014). MODIS time-series-derived indicators for the beginning of the growing season in boreal coniferous forest—A comparison with CO2 flux measurements and phenological observations in Finland. *Remote Sensing of Environment*, *140*, 625–638. https://doi.org/10.1016/j.rse.2013.09.022

Brooks, P. D., McKnight, D., & Elder, K. (2005). Carbon limitation of soil respiration under winter snowpacks: Potential feedbacks between growing season and winter carbon fluxes. *Global Change Biology*, *11*(2), 231–238. https://doi.org/10.1111/j.1365-2486.2004.00877.x

Byrne, B., Liu, J., Yi, Y., Chatterjee, A., Basu, S., Cheng, R., Doughty, R., Chevallier, F., Bowman, K. W., Parazoo, N. C., Crisp, D., Li, X., Xiao, J., Sitch, S., Guenet, B., Deng, F., Johnson, M. S., Philip, S., McGuire, P. C., & Miller, C. E. (2022). Multi-year observations reveal a larger than expected autumn respiration signal across northeast Eurasia. *Biogeosciences*, *19*(19), 4779–4799. https://doi.org/10.5194/bg-19-4779-2022

Byun, E., Rezanezhad, F., Fairbairn, L., Slowinski, S., Basiliko, N., Price, J. S., Quinton, W. L., Roy-Léveillée, P., Webster, K., & Van Cappellen, P. (2021). Temperature, moisture and freeze–thaw controls on CO2 production in soil incubations from northern peatlands. *Scientific Reports*, *11*(1), 23219. https://doi.org/10.1038/s41598-021-02606-3

Campeau, A., Vachon, D., Bishop, K., Nilsson, M. B., & Wallin, M. B. (2021). Autumn destabilization of deep porewater CO2 store in a northern peatland driven by turbulent diffusion. *Nature Communications*, *12*(1), 6857. https://doi.org/10.1038/s41467-021-27059-0

Commane, R., Lindaas, J., Benmergui, J., Luus, K. A., Chang, R. Y.-W., Daube, B. C., Euskirchen, E. S., Henderson, J. M., Karion, A., Miller, J. B., Miller, S. M., Parazoo, N. C., Randerson, J. T., Sweeney, C., Tans, P., Thoning, K., Veraverbeke, S., Miller, C. E., & Wofsy, S. C. (2017). Carbon dioxide sources from Alaska driven by increasing early winter respiration from Arctic tundra. *Proceedings of the National Academy of Sciences*, *114*(21), 5361–5366. https://doi.org/10.1073/pnas.1618567114

Friedlingstein, P., O'Sullivan, M., Jones, M. W., Andrew, R. M., Gregor, L., Hauck, J., Le Quéré, C., Luijkx, I. T., Olsen, A., Peters, G. P., Peters, W., Pongratz, J., Schwingshackl, C., Sitch, S., Canadell, J. G., Ciais, P., Jackson, R. B., Alin, S. R., Alkama, R., … Zheng, B. (2022). Global Carbon Budget 2022. *Earth System Science Data*, *14*(11), 4811–4900. https://doi.org/10.5194/essd-14-4811-2022

https://doi.org/10.5194/egusphere-2025-5778
Preprint. Discussion started: 11 December 2025

Gorham, E. (1991). Northern Peatlands: Role in the Carbon Cycle and Probable Responses to Climatic Warming. *Ecological Applications*, *1*(2), 182–195. https://doi.org/10.2307/1941811

Hugelius, G., Loisel, J., Chadburn, S., Jackson, R. B., Jones, M., MacDonald, G., Marushchak, M., Olefeldt, D., Packalen, M., Siewert, M. B., Treat, C., Turetsky, M., Voigt, C., & Yu, Z. (2020). Large stocks of peatland carbon and nitrogen are vulnerable to permafrost thaw. *Proceedings of the National Academy of Sciences*, *117*(34), 20438–20446. https://doi.org/10.1073/pnas.1916387117

Hugelius, G., Ramage, J., Burke, E., Chatterjee, A., Smallman, T. L., Aalto, T., Bastos, A., Biasi, C., Canadell, J. G., Chandra, N., Chevallier, F., Ciais, P., Chang, J., Feng, L., Jones, M. W., Kleinen, T., Kuhn, M., Lauerwald, R., Liu, J., … Zheng, B. (2024). Permafrost Region Greenhouse Gas Budgets Suggest a Weak CO2 Sink and CH4 and N2O Sources, But Magnitudes Differ Between Top-Down and Bottom-Up Methods. *Global Biogeochemical Cycles*, *38*(10), e2023GB007969. https://doi.org/10.1029/2023GB007969

Kollo, J., Metslaid, S., Padari, A., Hordo, M., Kangur, A., & Noe, S. M. (2023). Trends in thermal growing season length from years 1955–2020–A case study in hemiboreal forest in Estonia. *Boreal Environ Res*, *28*, 169-180.

Korrensalo, A., Mammarella, I., Alekseychik, P., Vesala, T., & Tuittila, E.-S. (2022). Plant mediated methane efflux from a boreal peatland complex. *Plant and Soil*, *471*(1), 375–392. https://doi.org/10.1007/s11104-021-05180-9

Korrensalo, A., Kettunen, J., Mehtätalo, L., Vanhatalo, J., & Tuittila, E.-S. (2025). Detecting Subtle Change in Species and Trait Composition and Quantifying Its Uncertainty in a Boreal Peatland. *Journal of Vegetation Science*, *36*(2), e70025. https://doi.org/10.1111/jvs.70025

Körner, C., Möhl, P., & Hiltbrunner, E. (2023). Four ways to define the growing season. *Ecology Letters*, *26*(8), 1277–1292. https://doi.org/10.1111/ele.14260

Kulmala, L., Pumpanen, J., Kolari, P., Dengel, S., Berninger, F., Köster, K., Matkala, L., Vanhatalo, A., Vesala, T., & Bäck, J. (2019). Inter- and intra-annual dynamics of photosynthesis differ between forest floor vegetation and tree canopy in a subarctic Scots pine stand. *Agricultural and Forest Meteorology*, *271*, 1–11. https://doi.org/10.1016/j.agrformet.2019.02.029

López-Blanco, E., Lund, M., Christensen, T. R., Tamstorf, M. P., Smallman, T. L., Slevin, D., Westergaard-Nielsen, A., Hansen, B. U., Abermann, J., & Williams, M. (2018). Plant Traits are Key Determinants in Buffering the Meteorological Sensitivity of Net Carbon Exchanges of Arctic Tundra. *Journal of Geophysical Research: Biogeosciences*, *123*(9), 2675–2694. https://doi.org/10.1029/2018JG004386

López-Blanco, E., Lund, M., Williams, M., Tamstorf, M. P., Westergaard-Nielsen, A., Exbrayat, J.-F., Hansen, B. U., & Christensen, T. R. (2017). Exchange of CO₂ in Arctic tundra: Impacts of meteorological variations and biological disturbance. *Biogeosciences*, *14*(19), 4467–4483. https://doi.org/10.5194/bg-14-4467-2017

López-Blanco, E., Väisänen, M., Salmon, E., Jones, C. P., Schmidt, N. M., Marttila, H., Lohila, A., Juutinen, S., Scheller, J., & Christensen, T. R. (2025). The net ecosystem carbon balance (NECB) at catchment scales in the Arctic. *Frontiers in Environmental Science*, *13*. https://doi.org/10.3389/fenvs.2025.1544586

https://doi.org/10.5194/egusphere-2025-5778
Preprint. Discussion started: 11 December 2025

Mammarella, I., Peltola, O., & Nordbo, A. (2016). EddyUH: an advanced software package for eddy covariance flux calculation for a wide range of instrumentation and ecosystems. *Atmospheric Measurement Techniques*, *2016*(1), 1.

Martz, F., Vuosku, J., Ovaskainen, A., Stark, S., & Rautio, P. (2016). The Snow Must Go On: Ground Ice Encasement, Snow Compaction and Absence of Snow Differently Cause Soil Hypoxia, CO2 Accumulation and Tree Seedling Damage in Boreal Forest. *PLOS ONE*, *11*(6), e0156620. https://doi.org/10.1371/journal.pone.0156620

Mastepanov, M., Sigsgaard, C., Tagesson, T., Ström, L., Tamstorf, M. P., Lund, M., & Christensen, T. R. (2013). Revisiting factors controlling methane emissions from high-Arctic tundra. *Biogeosciences*, *10*(7), 5139–5158. https://doi.org/10.5194/bg-10-5139-2013

Morgner, E., Elberling, B., Strebel, D., & Cooper, E. J. (2010). The importance of winter in annual ecosystem respiration in the High Arctic: Effects of snow depth in two vegetation types. *Polar Research*, *29*(1), 58–74. https://doi.org/10.1111/j.1751-8369.2010.00151.x

Natali, S. M., Watts, J. D., Rogers, B. M., Potter, S., Ludwig, S. M., Selbmann, A.-K., Sullivan, P. F., Abbott, B. W., Arndt, K. A., Birch, L., Björkman, M. P., Bloom, A. A., Celis, G., Christensen, T. R., Christiansen, C. T., Commane, R., Cooper, E. J., Crill, P., Czimczik, C., … Zona, D. (2019). Large loss of CO2 in winter observed across the northern permafrost region. *Nature Climate Change*, *9*(11), 852–857. https://doi.org/10.1038/s41558-019-0592-8

Nichols, J. E., & Peteet, D. M. (2019). Rapid expansion of northern peatlands and doubled estimate of carbon storage. *Nature Geoscience*, *12*(11), 917–921. https://doi.org/10.1038/s41561-019-0454-z

Pallandt, M. M. T. A., Kumar, J., Mauritz, M., Schuur, E. A. G., Virkkala, A.-M., Celis, G., Hoffman, F. M., & Göckede, M. (2022). Representativeness assessment of the pan-Arctic eddy covariance site network and optimized future enhancements. *Biogeosciences*, *19*(3), 559–583. https://doi.org/10.5194/bg-19-559-2022

Pongracz, A., Wårlind, D., Miller, P. A., Gustafson, A., Rabin, S. S., & Parmentier, F.-J. W. (2024). Warming-induced contrasts in snow depth drive the future trajectory of soil carbon loss across the Arctic-Boreal region. *Communications Earth & Environment*, *5*(1), 684. https://doi.org/10.1038/s43247-024-01838-1

Rafat, A., Byun, E., Rezanezhad, F., Quinton, W. L., Humphreys, E. R., Webster, K., & Van Cappellen, P. (2022). The definition of the non-growing season matters: A case study of net ecosystem carbon exchange from a Canadian peatland. *Environmental Research Communications*, *4*(2), 021003. https://doi.org/10.1088/2515-7620/ac53c2

Rantanen, M., Karpechko, A. Y., Lipponen, A., Nordling, K., Hyvärinen, O., Ruosteenoja, K., Vihma, T., & Laaksonen, A. (2022). The Arctic has warmed nearly four times faster than the globe since 1979. *Communications Earth & Environment*, *3*(1), 1–10. https://doi.org/10.1038/s43247-022-00498-3

Rantanen, M., Lee, S. H., & Aalto, J. (2023). Asymmetric warming rates between warm and cold weather regimes in Europe. *Atmospheric Science Letters*, *24*(10), e1178. https://doi.org/10.1002/asl.1178

Raz-Yaseef, N., Torn, M. S., Wu, Y., Billesbach, D. P., Liljedahl, A. K., Kneafsey, T. J., Romanovsky, V. E., Cook, D. R., & Wullschleger, S. D. (2017). Large CO2 and CH4 emissions from

https://doi.org/10.5194/egusphere-2025-5778
Preprint. Discussion started: 11 December 2025

polygonal tundra during spring thaw in northern Alaska. *Geophysical Research Letters*, *44*(1), 504–513. https://doi.org/10.1002/2016GL071220

Rinne, J., Riutta, T., Pihlatie, M., Aurela, M., Haapanala, S., Tuovinen, J.-P., Tuittila, E.-S., & Vesala, T. (2007). Annual cycle of methane emission from a boreal fen measured by the eddy covariance technique. *Tellus B: Chemical and Physical Meteorology*, *59*(3), 449–457. https://doi.org/10.1111/j.1600-0889.2007.00261.x

Rinne, J., Tuovinen, J.-P., Klemedtsson, L., Aurela, M., Holst, J., Lohila, A., Weslien, P., Vestin, P., Łakomiec, P., Peichl, M., Tuittila, E.-S., Heiskanen, L., Laurila, T., Li, X., Alekseychik, P., Mammarella, I., Ström, L., Crill, P., & Nilsson, M. B. (2020). Effect of the 2018 European drought on methane and carbon dioxide exchange of northern mire ecosystems. *Philosophical Transactions of the Royal Society B: Biological Sciences*, *375*(1810), 20190517. https://doi.org/10.1098/rstb.2019.0517

Riutta, T., Laine, J., & Tuittila, E.-S. (2007). Sensitivity of CO2 Exchange of Fen Ecosystem Components to Water Level Variation. *Ecosystems*, *10*(5), 718–733. https://doi.org/10.1007/s10021-007-9046-7

See, C. R., Virkkala, A.-M., Natali, S. M., Rogers, B. M., Mauritz, M., Biasi, C., Bokhorst, S., Boike, J., Bret-Harte, M. S., Celis, G., Chae, N., Christensen, T. R., Murner (Connon), S. J., Dengel, S., Dolman, H., Edgar, C. W., Elberling, B., Emmerton, C. A., Euskirchen, E. S., … Schuur, E. A. G. (2024). Decadal increases in carbon uptake offset by respiratory losses across northern permafrost ecosystems. *Nature Climate Change*, *14*(8), 853–862. https://doi.org/10.1038/s41558-024-02057-4

Sullivan, B. W., Dore, S., Montes-Helu, M. C., Kolb, T. E., & Hart, S. C. (2012). Pulse Emissions of Carbon Dioxide during Snowmelt at a High-Elevation Site in Northern Arizona, U.S.A. *Arctic, Antarctic, and Alpine Research*, *44*(2), 247–254. https://doi.org/10.1657/1938-4246-44.2.247

Virkkala, A.-M., Aalto, J., Rogers, B. M., Tagesson, T., Treat, C. C., Natali, S. M., Watts, J. D., Potter, S., Lehtonen, A., Mauritz, M., Schuur, E. A. G., Kochendorfer, J., Zona, D., Oechel, W., Kobayashi, H., Humphreys, E., Goeckede, M., Iwata, H., Lafleur, P. M., … Luoto, M. (2021). Statistical upscaling of ecosystem CO2 fluxes across the terrestrial tundra and boreal domain: Regional patterns and uncertainties. *Global Change Biology*, *27*(17), 4040–4059. https://doi.org/10.1111/gcb.15659

Virkkala, A.-M., Natali, S. M., Rogers, B. M., Watts, J. D., Savage, K., Connon, S. J., Mauritz, M., Schuur, E. A. G., Peter, D., Minions, C., Nojeim, J., Commane, R., Emmerton, C. A., Goeckede, M., Helbig, M., Holl, D., Iwata, H., Kobayashi, H., Kolari, P., … Zyryanov, V. I. (2022). The ABCflux database: Arctic–boreal CO_2 flux observations and ancillary information aggregated to monthly time steps across terrestrial ecosystems. *Earth System Science Data*, *14*(1), 179–208. https://doi.org/10.5194/essd-14-179-2022

Virkkala, A.-M., Wargowsky, I., Vogt, J., Kuhn, M. A., Madaan, S., O'Keefe, R., Windholz, T., Arndt, K. A., Rogers, B. M., Watts, J. D., Kent, K., Göckede, M., Olefeldt, D., Rocher-Ros, G., Schuur, E. A. G., Bastviken, D., Aalstad, K., Aho, K., Ala-Könni, J., … Natali, S. M. (2025). ABCFlux v2: Arctic–boreal CO_2 and CH_4 monthly flux observations and ancillary information across terrestrial and freshwater ecosystems. *Earth System Science Data Discussions*, 1–86. https://doi.org/10.5194/essd-2025-585

https://doi.org/10.5194/egusphere-2025-5778
Preprint. Discussion started: 11 December 2025

Wang, H., Yu, L., Chen, L., Zhang, Z., Li, X., Liang, N., Peng, C., & He, J.-S. (2023). Carbon fluxes and soil carbon dynamics along a gradient of biogeomorphic succession in alpine wetlands of Tibetan Plateau. *Fundamental Research*, *3*(2), 151–159. https://doi.org/10.1016/j.fmre.2022.09.024

Watts, J. D., Farina, M., Kimball, J. S., Schiferl, L. D., Liu, Z., Arndt, K. A., Zona, D., Ballantyne, A., Euskirchen, E. S., Parmentier, F.-J. W., Helbig, M., Sonnentag, O., Tagesson, T., Rinne, J., Ikawa, H., Ueyama, M., Kobayashi, H., Sachs, T., Nadeau, D. F., … Oechel, W. C. (2023). Carbon uptake in Eurasian boreal forests dominates the high-latitude net ecosystem carbon budget. *Global Change Biology*, *29*(7), 1870–1889. https://doi.org/10.1111/gcb.16553

Wei, J., Li, X., Liu, L., Christensen, T. R., Jiang, Z., Ma, Y., Wu, X., Yao, H., & López-Blanco, E. (2022). Radiation, soil water content, and temperature effects on carbon cycling in an alpine swamp meadow of the northeastern Qinghai–Tibetan Plateau. *Biogeosciences*, *19*(3), 861–875. https://doi.org/10.5194/bg-19-861-2022

Yao, H., Peng, H., Hong, B., Guo, Q., Ding, H., Hong, Y., Zhu, Y., Cai, C., & Chi, J. (2022). Environmental Controls on Multi-Scale Dynamics of Net Carbon Dioxide Exchange From an Alpine Peatland on the Eastern Qinghai-Tibet Plateau. *Frontiers in Plant Science*, *12*. https://doi.org/10.3389/fpls.2021.791343

Yu, Z., Beilman, D. W., Frolking, S., MacDonald, G. M., Roulet, N. T., Camill, P., & Charman, D. J. (2011). Peatlands and Their Role in the Global Carbon Cycle. *Eos, Transactions American Geophysical Union*, *92*(12), 97–98. https://doi.org/10.1029/2011EO120001